Paradigm Academic Press
Innovation in Science and Technology
ISSN 2788-7030
JUL. 2023 VOL.2, NO.4

Microstructure Evolution in Medium Carbon Bainitic Steel

J N Mohapatra[1], D Satish Kumar[1] & G Balachandran[1]

[1] JSW Steel Ltd, Toranagallu, Bellary, Karnataka 583275, India

Correspondence: J N Mohapatra, JSW Steel Ltd, Toranagallu, Bellary, Karnataka 583275, India.

doi:10.56397/IST.2023.07.02

Abstract

A 0.38C steel with 1.97Mn, 1.34Si, 0.8Cr and 0.29Mo (wt. %) bainitic steel melted in a lab scale induction furnace was hot forged and subjected to annealing, austenitizing above Ac_3 temperature and in the inter critical temperature range were normalized or austempered in the temperature between 350 to 500 ^oC to get a versatile range of microstructure with bainite as a major phase. In the annealed condition the steel showed acicular ferrite with pearlite and in the normalized condition from above Ac_3 temperature, bainitic ferrite with 7% retained austenite. When the steel is continuously cooled post intercritical austenitization treatment, the microstructure showed ferrite, bainite and pearlite. Austenitization above Ac_3, followed by austempering at different temperatures resulted in carbide free bainitic microstructure consisting of bainitic ferrite and austenite between 7 and 16%. Austenitization in the inter critical temperature followed by austempering at different temperatures showed ferrite, banitic carbide and pearlite.

Keywords: Bainitic steel, continuous cooling, carbide free bainite, TRIP assisted steel

1. Introduction

Studies on low alloy TRIP assisted steels is centered around steels with carbon content about 0.2% to ensure good weldability and formability; Si greater than 1.5% to suppress the cementite formation, Mn between 1.5 to 2.5 % to enhance hardenability (I Samajdar, E Girault, B Verlinden, E Aernoudt & J Van, 1998; Arif Basuki & Etienne Aernoudt, 1999; K Sugimoto, A Kanda, R Kikuchi, S Hashimoto, T Kashima & S Ikeda, 2002; S Nemecek, Z Novy & H Stankov, 2006; J Zrnik, O Muransky, P Lukas, Z Novy, P Sittner & P Hornak, 2006; O Muransky, P Hornak, P Lukas, J Zrník & P Sittner, 2006; R Petrov, L Kestens, A Wasilkowska, & Y Houbaert, 2007; J Zrnik, O Stejskal, Z Novy, P Hornak & M Fujda, 2007; J Zrnik, O Muransky, O Stejskal, P Lukas & P Hornak, 2008; S Wen, L Lin, B C De Cooman, P Wollants & Y Chun-xia, 2008; B Masek, H Stan Kova, Z Novy, L W Meyer & A Kraci, 2009; T B Hilditch, I B Timokhina, L T Robertson, E V Pereloma, & P D Hodgson, 2009; L C Zhang, I B Timokhina, A La Fontaine, S P Ringer, P D Hodgson & E V Pereloma, 2009; M E Mehtedi, S Spinarelli & J Zrnik, 2010; J C Hell, M Dehmas, S Allain, J M Prado, A Hazotte & J P Chateau, 2011; H Asmari, E Emadoddin & A Habibolahzade, 2012, K Hausmann, D Krizan, & A Pichle, A Werner, 2013; F G Caballero, S Allain, J Cornide, J D Puerta Velasquez, C Garcia-Mateo & M K Miller, 2013; I Timokhina, E Pereloma, & P Hodgson, 2014; C Hofer, H Leitner, F Winkelhofer, H Clemens & S Primig, 2015; C Hofer, F Winkelhofer, J Krammerbauer, H Clemensa & S Primig, 2015, L Kucerova, M Bystriansky, 2016; Z P Xiong, A G Kostryzhev, L Chen & EV Pereloma, 2016; M Breuer, M Degner, G Bader, W Bleck & F Morganti, 2017; M Zhou, G Xu, J Tian, H Hu & Q Yuan, 2017; W Bleck, X Guo & M Yan, 2017; L Liu, B He & M Huang, 2018; G Gao, B Bai, H Zhang, X Gui, Z Tan & Y Weng, 2019; S Tang, H Lan, Z Liu & G Wang, 2021). In addition, steels are alloyed

with Cr and Mo (J C Hell, M Dehmas, S Allain, J M Prado, A Hazotte & J P Chateau, 2011; H Asmari, E Emadoddin & A Habibolahzade, 2012; K Hausmann, D Krizan, A Pichle & A Werner, 2013; F G Caballero, S Allain, J Cornide, J D Puerta Velasquez, C Garcia-Mateo & M K Miller, 2013; L Kucerova & M Bystriansky, 2016; Z P Xiong, A G Kostryzhev, L Chen & EV Pereloma, 2016), enhance the lower bainite formation that result in improved properties; in some cases Ni (J A Rodriguez-Martinez, R Pesci, A Rusinek, A Arias, R Zaera & D A Pedroche, 2010) and very small Cu (J Zrnik, O Muransky, P Lukas, Z Novy, P Sittner & P Hornak, 2006; O Muransky, P Hornak, P Lukas, J Zrník & P Sittner, 2006; R Petrov, L Kestens, A Wasilkowska, & Y Houbaert, 2007; J Zrnik, O Stejskal, Z Novy, P Hornak & M Fujda, 2007; J Zrnik, O Muransky, O Stejskal, P Lukas & P Hornak, 2008; B Masek, H Stan Kova, Z Novy, L W Meyer & A Kraci, 2009; T B Hilditch, I B Timokhina, L T Robertson, E V Pereloma, & P D Hodgson, 2009; L C Zhang, I B Timokhina, A La Fontaine, S P Ringer, P D Hodgson & E V Pereloma, 2009; M E Mehtedi, S Spinarelli & J Zrnik, 2010; F G Caballero, S Allain, J Cornide, J D Puerta Velasquez, C Garcia-Mateo & M K Miller, 2013; I Timokhina, E Pereloma, & P Hodgson, 2014; Z P Xiong, A G Kostryzhev, L Chen & EV Pereloma, 2016; J A Rodriguez-Martinez, R Pesci, A Rusinek, A Arias, R Zaera, D A Pedroche, 2010) additives have been made that enhance austenite stability and hardenability. The grain refinement in the steels are achieved by addition of Nb (S Nemecek, Z Novy & H Stankov, 2006; J Zrnik, O Muransky, P Lukas, Z Novy, P Sittner & P Hornak, 2006; O Muransky, P Hornak, P Lukas, J Zrník & P Sittner, 2006; J Zrnik, O Stejskal, Z Novy, P Hornak & M Fujda, 2007; J Zrnik, O Muransky, O Stejskal, P Lukas & P Hornak, 2008; B Masek, H Stan Kova, Z Novy, L W Meyer & A Kraci, 2009; M E Mehtedi, S Spinarelli & J Zrnik, 2010, H Asmari, E Emadoddin & A Habibolahzade, 2012; K Hausmann, D Krizan, &A Pichle, A Werner, 2013; L Kucerova, M Bystriansky, 2016; G Gao, B Bai, H Zhang, X Gui, Z Tan & Y Weng, 2019), and Ti, which resulted in improved properties as well. The microstructure targeted is either a carbide free bainitic microstructure where the steel is heated to above Ac_3 temperature, quenched to bainitic bay and held to form a lamellar structure of ferrite and retained austenite as lamellae (J C Hell, M Dehmas, S Allain, J M Prado, A Hazotte & J P Chateau, 2011; F G Caballero, S Allain, J Cornide, J D Puerta Velasquez, C Garcia-Mateo & M K Miller, 2013). TRIP assisted steel involves a holding treatment in the inter critical temperature range followed by baintic bay holding. The microstructure has polygonal ferrite, bainitic ferrite as major phases along with retained austenite and martensite-austenite constituents (I Samajdar, E Girault, B Verlinden, E Aernoudt & J Van, 1998; Arif Basuki & Etienne Aernoudt, 1999; K Sugimoto, A Kanda, R Kikuchi, S Hashimoto, T Kashima & S Ikeda, 2002; S Nemecek, Z Novy & H Stankov, 2006; J Zrnik, O Muransky, P Lukas, Z Novy, P Sittner & P Hornak, 2006; O Muransky, P Hornak, P Lukas, J Zrník & P Sittner, 2006; R Petrov, L Kestens, A Wasilkowska, & Y Houbaert, 2007; J Zrnik, O Stejskal, Z Novy, P Hornak & M Fujda, 2007; J Zrnik, O Muransky, O Stejskal, P Lukas & P Hornak, 2008; S Wen, L Lin, B C De Cooman, P Wollants & Y Chun-xia, 2008; B Masek, H Stan Kova, Z Novy, L W Meyer & A Kraci, 2009; T B Hilditch, I B Timokhina, L T Robertson, E V Pereloma, & P D Hodgson, 2009; L C Zhang, I B Timokhina, A La Fontaine, S P Ringer, P D Hodgson & E V Pereloma, 2009; M E Mehtedi, S Spinarelli & J Zrnik, 2010; J C Hell, M Dehmas, S Allain, J M Prado, A Hazotte & J P Chateau, 2011; H Asmari, E Emadoddin & A Habibolahzade, 2012; K Hausmann, D Krizan, &A Pichle, A Werner, 2013; F G Caballero, S Allain, J Cornide, J D Puerta Velasquez, C Garcia-Mateo & M K Miller, 2013; I Timokhina, E Pereloma, & P Hodgson, 2014; C Hofer, H Leitner, F Winkelhofer, H Clemens & S Primig, 2015; C Hofer, F Winkelhofer, J Krammerbauer, H Clemensa & S Primig, 2015; L Kucerova, M Bystriansky, 2016; Z P Xiong, A G Kostryzhev, L Chen & EV Pereloma, 2016; M Breuer, M Degner, G Bader, W Bleck & F Morganti, 2017; M Zhou, G Xu, J Tian, H Hu & Q Yuan, 2017; W Bleck, X Guo & M Yan, 2017; L Liu, B He & M Huang, 2018; G Gao, B Bai, H Zhang, X Gui, Z Tan & Y Weng, 2019; S Tang, H Lan, Z Liu & G Wang, 2021). The volume percentage of the phases are influenced by the steel chemistry, austenitizing condition and bainitic bay holding temperature. Further, low temperature thermomechanical processing especially intercritical deformation enhances the retained austenite content which improves the mechanical properties (J Zrnik, O Stejskal, Z Novy,

P Hornak & M Fujda, 2007).

There are studies on medium carbon (0.2%) along with Cr improves the formation bainite. Still higher carbon is expected to promote much improved carbide free bainite. The presence of Si on modifying the cementite in the conventional annealing has not been explored in any studies. Also, the conventional normalizing heat treatments, on high Si C-Mn steel forms carbide free bainitie. In addition, the response of such steel to normalizing from intercritical annealing has not well explored. Along with austempering above Ac_3 and in comparison from intercritical annealing is of interest to explore. This study is mainly focused on the microstructure evolution in the steel at all these thermal processing conditions.

2. Experimental

In the present study, the steel was made in a laboratory scale air induction melting unit, forged at JSW Steel Salem. The initial heat was 15 kg cast at 120 mm diameter ingot in metallic mould using low carbon steel and ferroalloys. The pipe portion of the solidified ingot was removed and hammer forged in one ton press in a laboratory forge press by heating the ingot to 1150 ºC and soaking it for 6 hours. The steel was reheated four times, when the temperature of the job falls below 850 ºC by measuring in a hand held pyrometer. The as-forged steel developed many fine cracks during forging. The cracked portion was discarded and an useful sound material was taken for experiment.

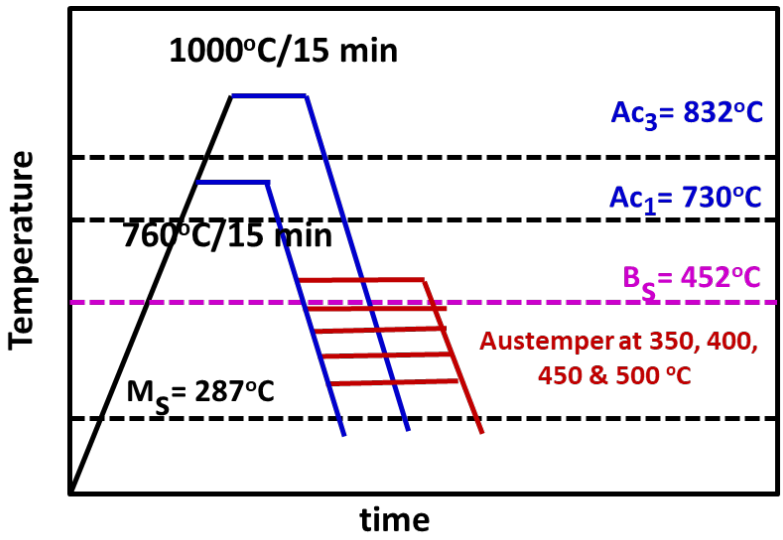

Figure 1. Heat treatment cycles carried out on the annealed steel

In the as forged and air cooled condition, the steels were very hard. Hence, the steel was subjected to annealing by heating the steel to 870 ºC holding for 60 min followed by furnace cooling. The annealed steel was used for further studies. The steel was evaluated in the annealed condition as a starting condition. The annealed steel was cut into sample of dimension 30 x 30 x 3 mm^3 for thermal treatment as per the cycles shown in Figure 1.

The steel samples were heated to 760ºC (inter critical) and 1000ºC (above A_{c3}), held for 15 min followed by continuous cooling to room temperature in air (normalizing). The samples were also used for austempering after austenization at the above two temperatures, held for 15 min at each condition followed by quenching the sample in a laboratory salt bath held at temperature of 350, 400, 450, and 500 ºC and holding time 30 min followed by air cooling. The heat treated samples were examined for their microstructure and hardness with selected ones used for phase analysis by XRD.

All the heat treatments and characterizations were carried out in the facilities at JSW Steel Ltd., Vijayanagar. The chemical analysis of the steel was analyzed using ARL Model ARL 3460 spectrometer. The hardness was measured using Zwick/Roell make (model: ZHμ). The optical microstructures were examined using Olympus make (Model: DSX-HRSU) opto-digital microscope. The scanning electron microscopy was carried out using Hitachi make (Model: S3400N) machine. The XRD analysis was carried out using PANalytical-Empyrean model. The tensile tests were carried out on a Zwick make 250kN Machine.

3. Results & Discussion

3.1 Chemical Composition and Theoretical Calculations for Transformation Temperatures, Phase Diagram, TTT

Diagram and T_0, T_0' Temperatures and Bainite Volume Fraction

Chemical composition of the steel is shown in Table 1, has a medium carbon content of 0.38% C. Carbon promotes the formation of bainite with high strength levels. The steel is alloyed with 1.97% Mn. The Mn content decreases the A_1 temperature and enlarges the austenite stability range. Thus, larger austenite phase fraction can be promoted at lower austenitizing temperature by increased Mn addition. The steel has 1.34% Si, which has a tendency to suppress the carbide formation and promote the formation of retained austenite. The steel is additionally alloyed with 0.8% Cr which has been reported to promote carbide free bainitic microstructure with a superior range of strength.

Table 1. Composition of the steel with transformation temperatures.

	C	**Mn**	**Si**	**S**	**P**	**Cr**	**Mo**	**Al**	**Ni**	**Cu**	**N**
Steel	0.38	1.97	1.34	0.006	0.018	0.80	0.29	0.033	0.03	0.024	95.09
Ac_1=730; Ac_3=832; B_s=452; M_s=287											
Ref (J Trzaska, 2016):											
Ac_1 =742 -29 %C -14 %Mn +13 %Si +16 %C r-17 %Ni -16 %Mo +45 %V +36 %Cu											
Ac_3 =925 -219 %SQRT(%C) -7 %Mn +39 %Si -16 %Ni +13 %Mo +97 %V											
B_s =771 -231.5 %C -69 %Mn -23 %Si -58.5 %Cr -31 %Ni-55 %Mo -41 %V											
M_s =541 -401 %C -36 %Mn -10.5 %Si -14 %Cr -18 %Ni -17 %Mo											

The Pseudo binary phase diagram of the steel as a function of carbon content is shown in Figure 2. The phase diagram shows the equilibrium phase stability, Ac_1 and Ac_3 can be studied from it. For the given carbon content, the equilibrium phases can be found for the chosen austenitization temperature in the inter-critical range.

It is well known that the bainitic transformation is displacive and is governed by an incomplete reaction phenomenon (F G Caballero, S Allain, J Cornide, J D Puerta Velasquez, C Garcia-Mateo & M K Miller, 2013; F G Caballero, M J Santofimia, C Capdevila, C Garcia-Mateo and C G de Andres, 2006). The TTT diagram for the given steel was developed using the Cambridge University Software MUCG83 (MUCG83 Cambridge Univ software, n.d.). Alloying with Cr and Mo has ensured that the bainitic bay enlarged. There is a potential to form bainite in moderate cooling rate. The B_s and M_s temperature obtained from the software and from the empirical equations in given in Table 1.

For better formability and weldability the carbon content is generally restricted to 0.25%. In the present study slightly higher carbon content is used considering its better response to bainitic reaction (Arif Basuki & Etienne Aernoudt, 1999; K Sugimoto, A Kanda, R Kikuchi, S Hashimoto, T Kashima & S Ikeda, 2002; S Nemecek, Z Novy & H Stankov, 2006; G Gao, B Bai, H Zhang, X Gui, Z Tan & Y Weng, 2019). The steel developed is alloyed suitably to have a low A_{c3} temperature to ensure full austenitization during annealing. The steel has to be sufficiently alloyed to get adequate hardenability and suppression of proeutectoid ferrite, when cooled after annealing. Addition of Si or Al or a mixture of both to a tune of 1.5% suppresses the cementite formation. However, the addition of Al raises the Ac_3 temperature and addition of Si does not favour formation of quality galvanized sheet surface. Addition of Cr and Mo to the steel promotes the lower bainite formation (J C Hell, M Dehmas, S Allain, J M Prado, A Hazotte & J P Chateau, 2011, K Hausmann, D Krizan, & A Pichle, A Werner, 2013; F G Caballero, S Allain, J Cornide, J D Puerta Velasquez, C Garcia-Mateo & M K Miller, 2013; C Hofer, F Winkelhofer, J Krammerbauer, H Clemensa & S Primig, 2015; L Kucerova, M Bystriansky, 2016; M Breuer, M Degner, G Bader, W Bleck & F Morganti, 2017; W Bleck, X Guo & M Yan, 2017).

The alloy system is in general based on (0.15-0.3) C-1.5Si-Mn-Cr (wt. %) (F G Caballero, M J Santofimia, C Capdevila, C Garcia-Mateo & C G de Andres, 2006). Bainitic transformation is a displacive transformation which grows tiny platelets of sub units of ferrite. The carbon solubility of ferrite is low, and the excess carbon rejected by these platelets is partitioned into the residual austenite around the plates after growth of the platelets. The carbon content limits the growth of the bainitic platelets at a temperature T_0'. While a temperature T_0 decides the composition at which the ferrite and austenite have the same free energy in a composition vs temperature plot, the T_0' takes into account the strain associated with the transformation. The TTT diagram for the steel studied is shown in Figure 3. The T_0 and T_0' was calculated for the given composition as shown in Figure 4, using the Cambridge University Software MUCG83.

The maximum volume fraction of bainite, $V_{B\text{-}max}$, which can be formed at a given temperature is directly related to the T_0' curve and can be calculated by mass balance of the equilibrium phases. The volume fraction of bainite,

V_B, formed at a given temperature is related to the T_0' and the mole fraction at the T_0 temperature,

$V_B = (x_\gamma - \text{x-bar}) / (x_\gamma - s)$

Where x_γ = carbon content of austenite according to the T_0 curve

x-bar = average carbon content of the alloy

s = amount of carbon trapped in the bainitic ferrite in solid solution (s = 0.03 wt.%)

The maximum volume fraction of bainite formed at a given transformation temperature will be a function of austempering temperature as shown in Figure 5.

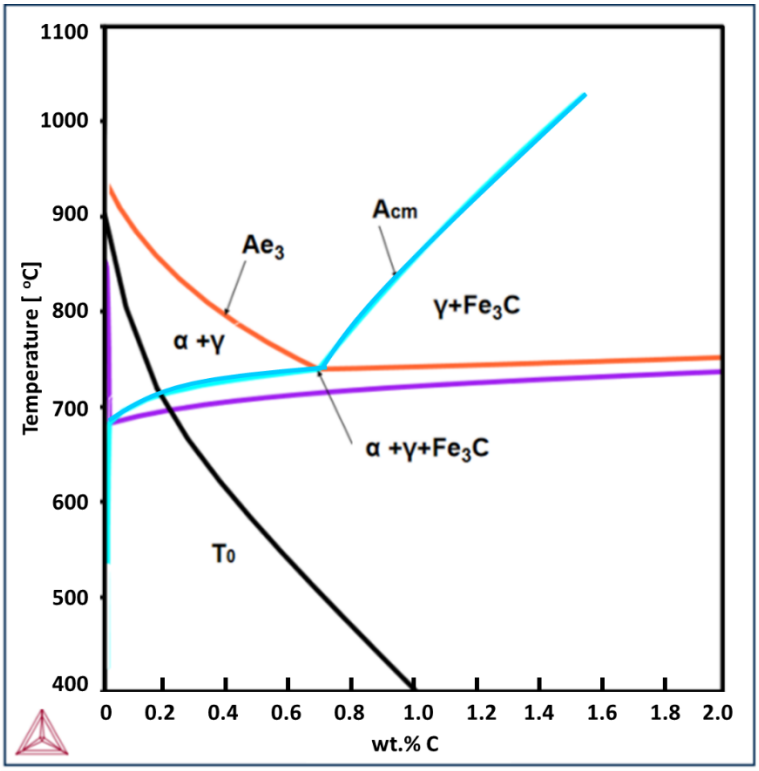

Figure 2. Pseudo-binary phase diagram of the steel as a function of carbon content

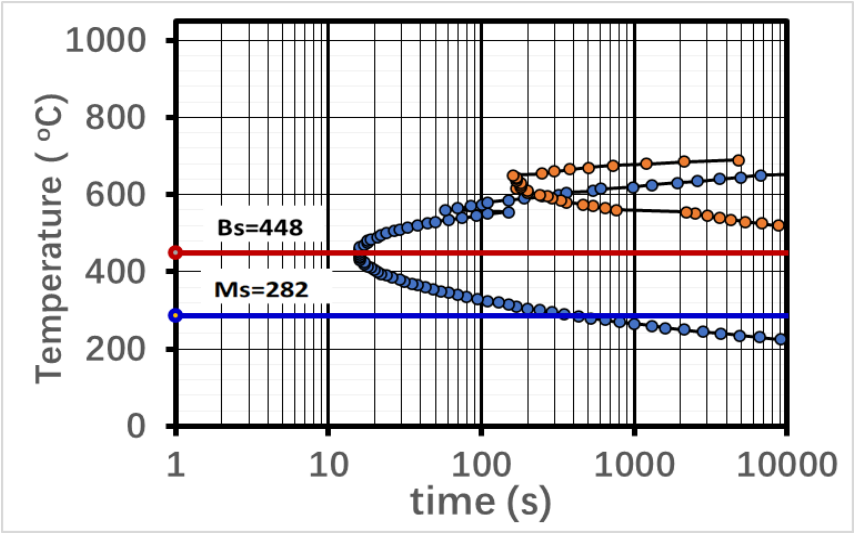

Figure 3. TTT diagram of the steel evolved based on Cambridge university software MUCG83

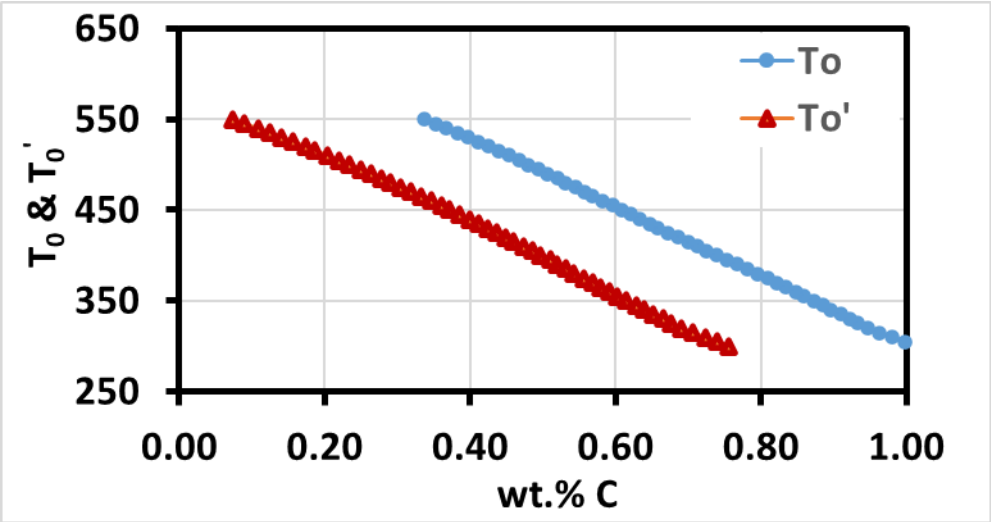

Figure 4. T_0 and T_0' of the steel over a range of composition from MUGC83

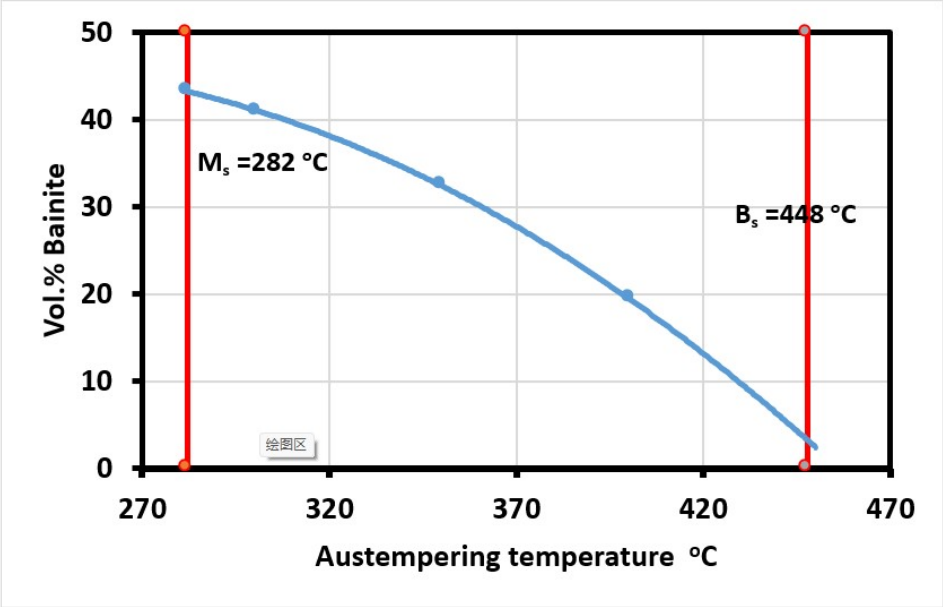

Figure 5. Maximum volume of bainite as a function of austempering temperature

3.2 Annealing Condition

The annealed sample optical image shows a microstructure that consists of bainite and pearlite (Figure 6(a)) with a hardness of 277 HV. SEM micrograph shows tendency to fine carbide formation closer to the grain boundaries (Figure 6(b)). Unlike the lamellar pearlite, expected in a normal annealed condition, the carbide appears as vermiculite morphology. Hence, the phases consisted of dispersed cementite along with bainite. The ferrite regions in the steel appear as acicular ferrite along with the regions of bainite. In the annealed condition, the steel shows mixed microstructure of pearlite, bainite and acicular ferrite. The presence of coarse lamellar pearlite increases hardness but the lamellar pearlite can lead to lower toughness. The XRD phase analysis shows a ferritic matrix and absence of retained austenite.

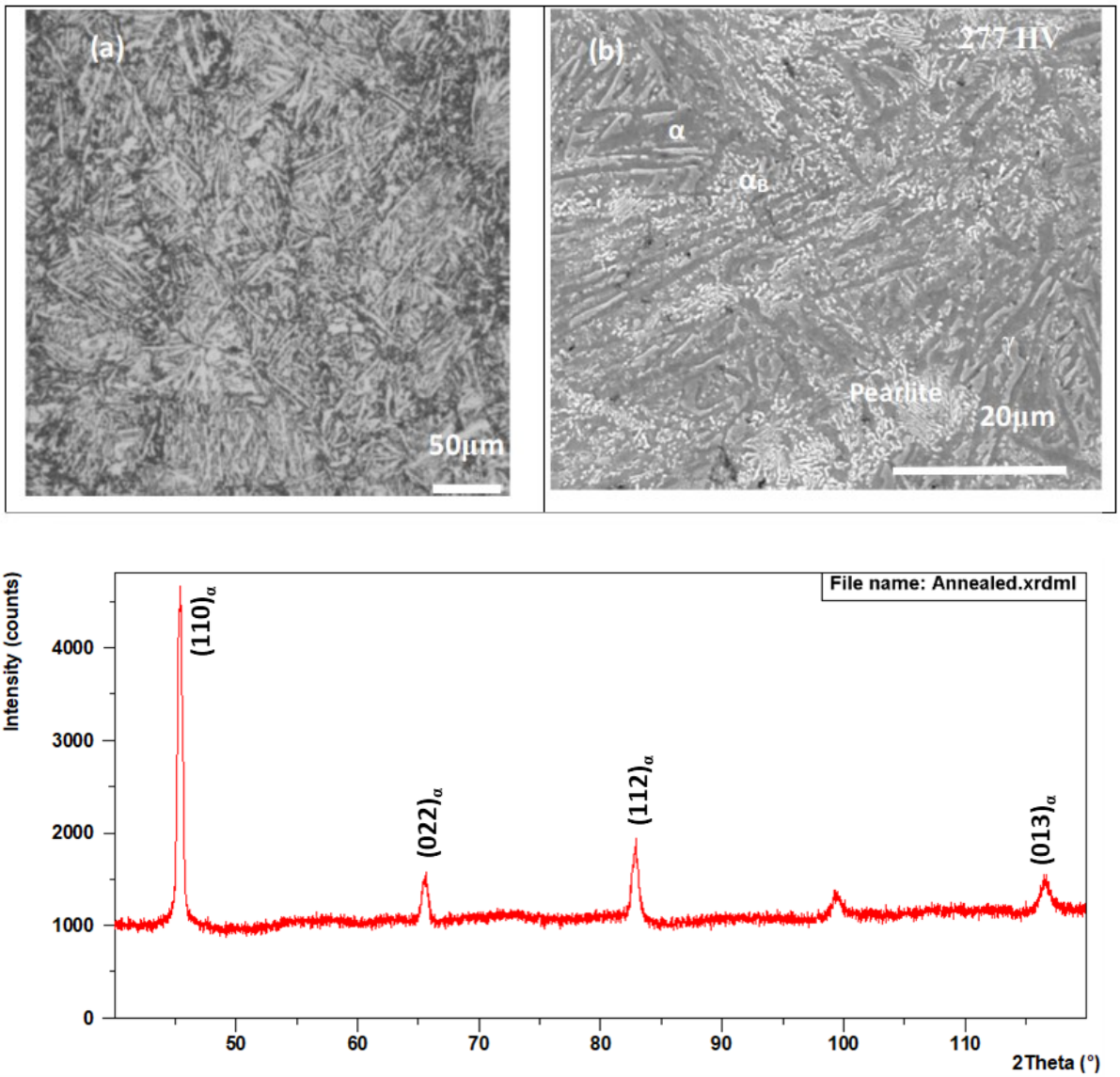

Figure 6. Microstructure of the steel in the annealed condition (870 ºC / 1 h / FC) (a) Optical microstructure (a) SEM micrograph (c) XRD analysis

3.3 Normalizing Above Ac_3

The steel when subjected to austenitizing above A_{c3} temperature at 1000 ºC, dissolves all the carbides. Faster cooling in ambient air is expected to produce fully ferrite - pearlite microstructure as shown in Figure 7.

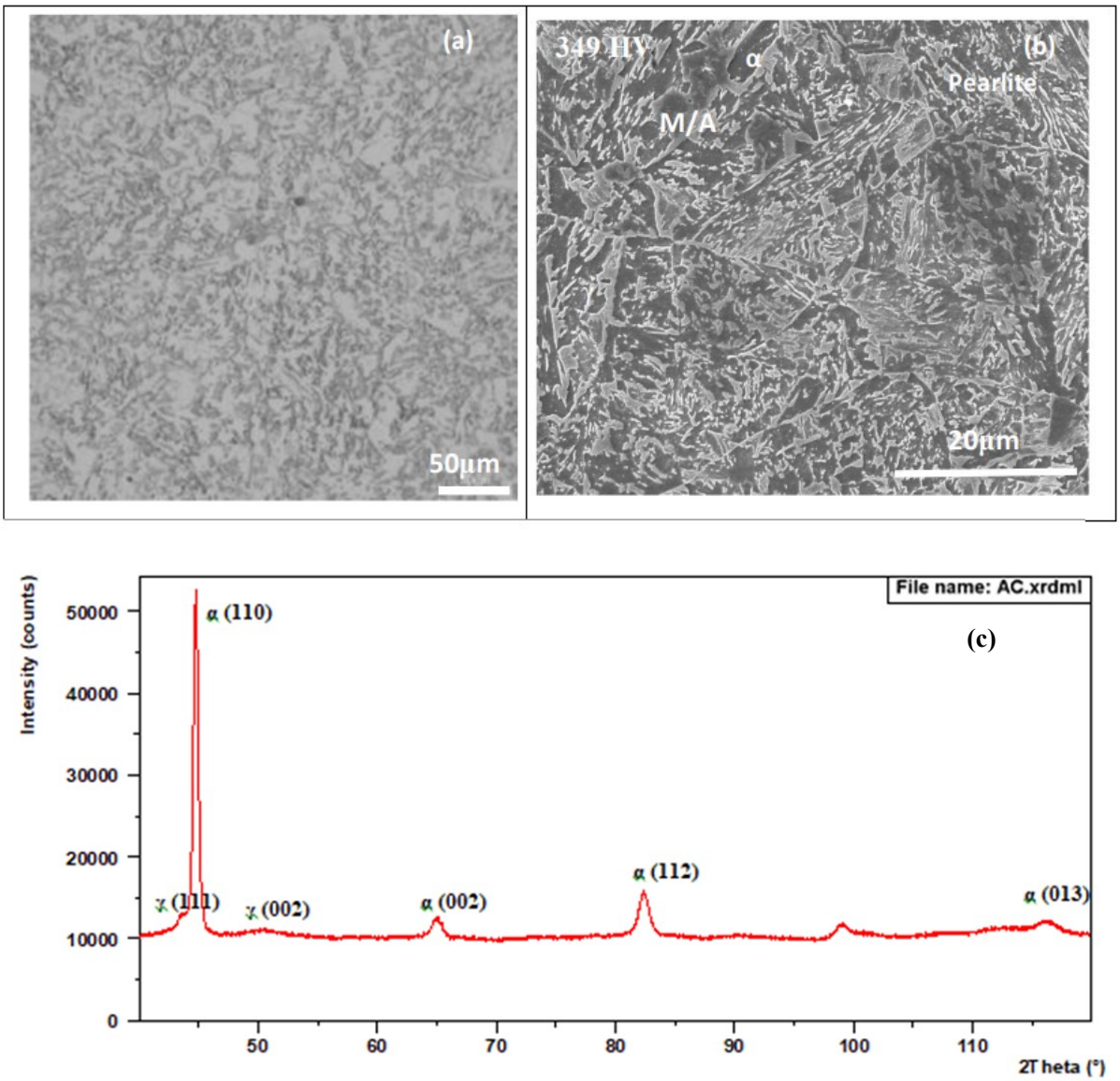

Figure 7. Microstructure of the steel in the normalized condition (1000 ºC/ 15 min/AC) (a) Optical microstructure (b) SEM microstructure (c) Typical XRD phase analysis shows 7% retained austenite

A dense distribution of fine pearlite along with some amount of bainite is formed. Due to the fine pearlite distribution compared to annealed condition the hardness after normalizing is found to be much higher (349 HV). The steel in this condition had a retained austenite content of about 7%. Hence, good plasticity properties can be expected. The wear resistance may be enhanced by the pearlite and the TRIP effect caused by the retained austenite. The reason for the existence of pearlite in the matrix could be due to the initial annealing treatment. The pearlite formed in the annealed condition probably could not completely dissolve. The microstructures with pearlite, ferrite and retained austenite are not reported in literature. The hardness value is 349 HV and hence both presence of pearlite and retained austenite together may improve the wear resistance property especially in applications such as rails.

3.4 Normalizing Post Intercritical Austenitizing

Normalizing treatment was carried out, post inter-critical austenitization in the steel. Accordingly, the 760ºC austenitization generates 66% austenite and 34% ferrite, with its carbon content enriched to 0.76%, which is near eutectoid composition, but slightly on the hypereutectoid side in the phase diagram in Figure 2. Air cooling this steel after the intercritical holding, promoted intercritical polygonal ferrite in regions of fine pearlite and bainitic ferrite dispersion are seen in Figure 8. Islands of the intercritical ferrite, is seen in the microstructure. The ferrite phase promotes softness in the steel and a hardness of 233 HV was observed. The XRD analysis shows predominantly ferrite without retained austenite. As the carbides are getting precipitated from the carbon enriched austenite, there is formation of bainitic ferrite. The residual presence of pearlite is probably due to

reprecipitation of pearlite and bainite from the austenite. Thus, ferrite, pearlite and fine bainitic ferrite is observed in the microstructure.

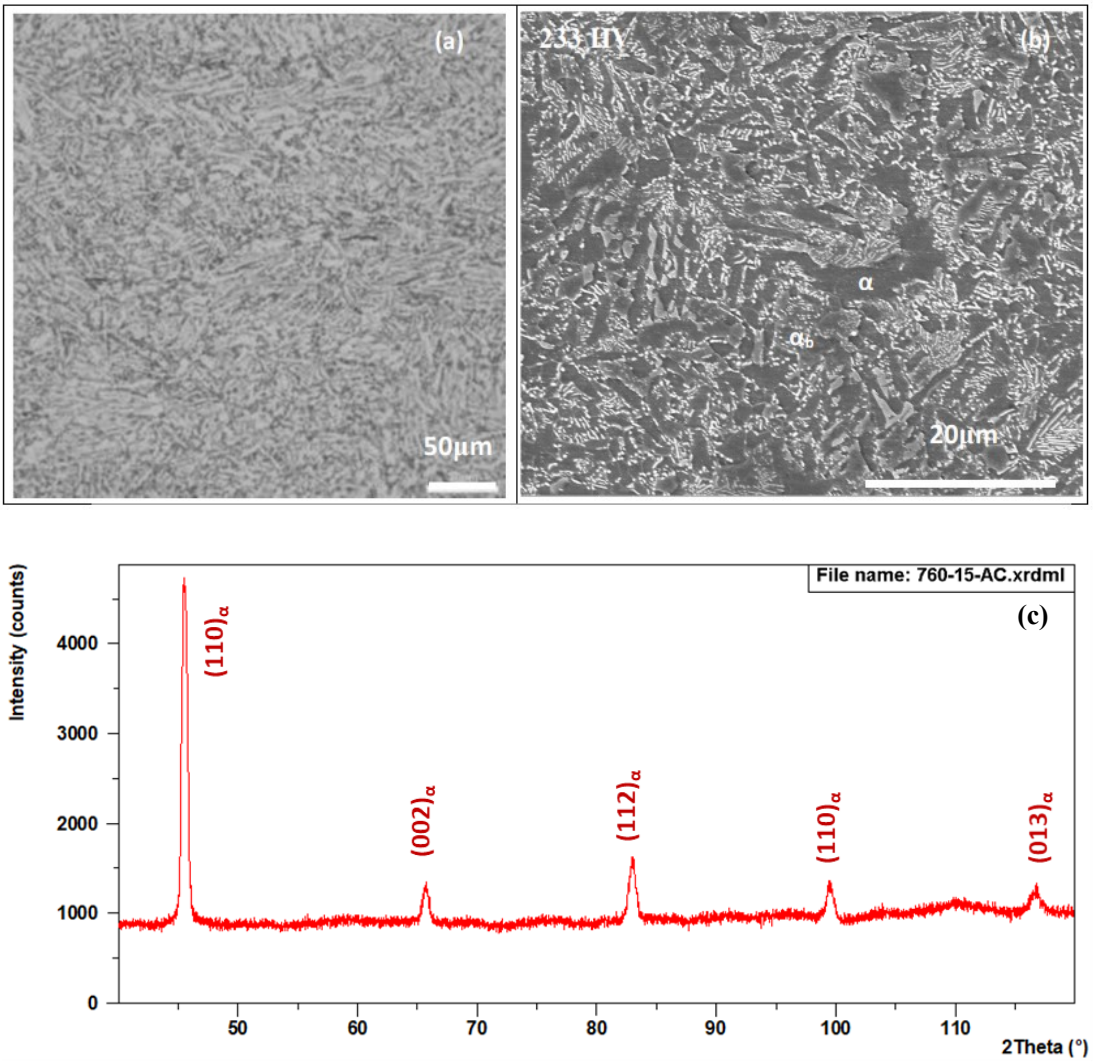

Figure 8. Microstructure of the steel intercritically austenitized (760 C for 15 min/AC) (a) Optical microstructure (b) SEM micrograph (c) XRD phase analysis.

3.5 Austempered from Above A_{c3} Condition Forming Carbide Free Bainitic Steels

Austempering the steel above A_{c3} promotes carbide free bainite in high silicon low alloy steel. In the present case austenitization at 1000ºC with 15 min holding followed by austempering between 350 and 500ºC in a molten salt bath followed by air cooling showed excellent lower bainite (LB) microstructure. The optical microstructures consisting of sheaves of carbide free bainite as in Figure 9 (M Zhou, G Xu, J Tian, H Hu & Q Yuan, 2017). The corresponding SEM microstructure in Figure 10 showed bainite sheaves with alternate layers of ferrite and thin film of austenite characteristic of carbide free bainitic microstructure. There are also regions of blocky M/A constituent in the microstructure and minimization of this is very important to realize the full benefit of the carbide free bainite microstructure.

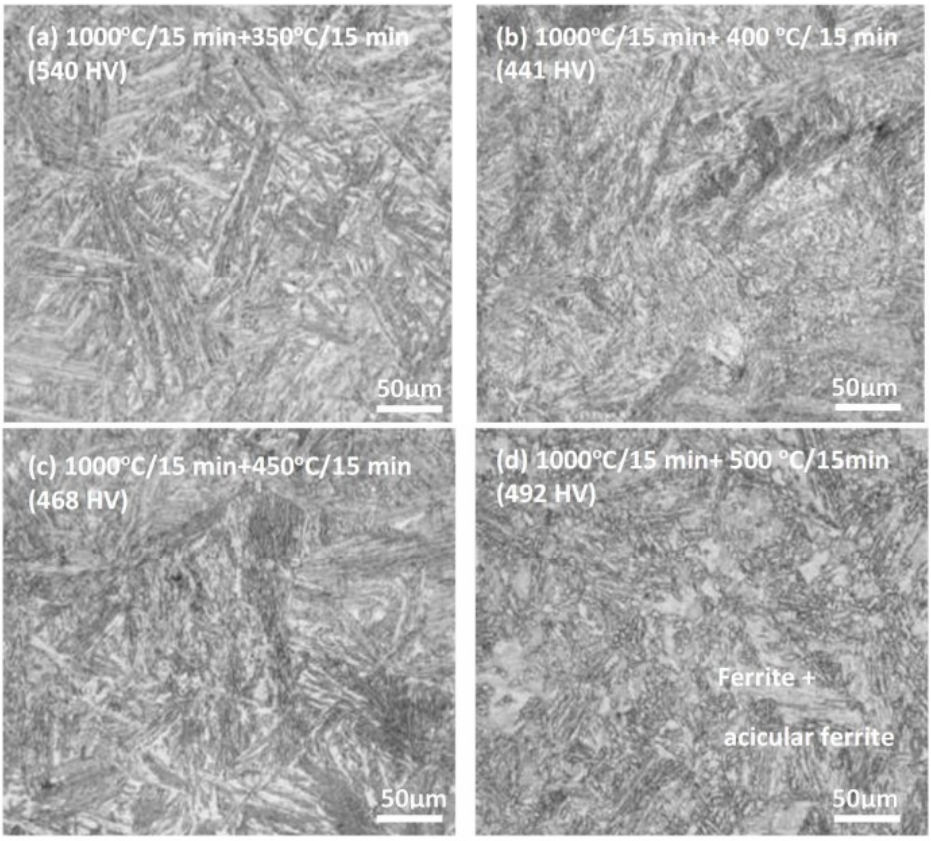

Figure 9. Microstructure of steels austenitized above A_3 at 1000ºC for 15 min/ austempering for 30 min in salt bath at (a) 350ºC (b) 400 ºC (c) 450 ºC (d) 500 ºC

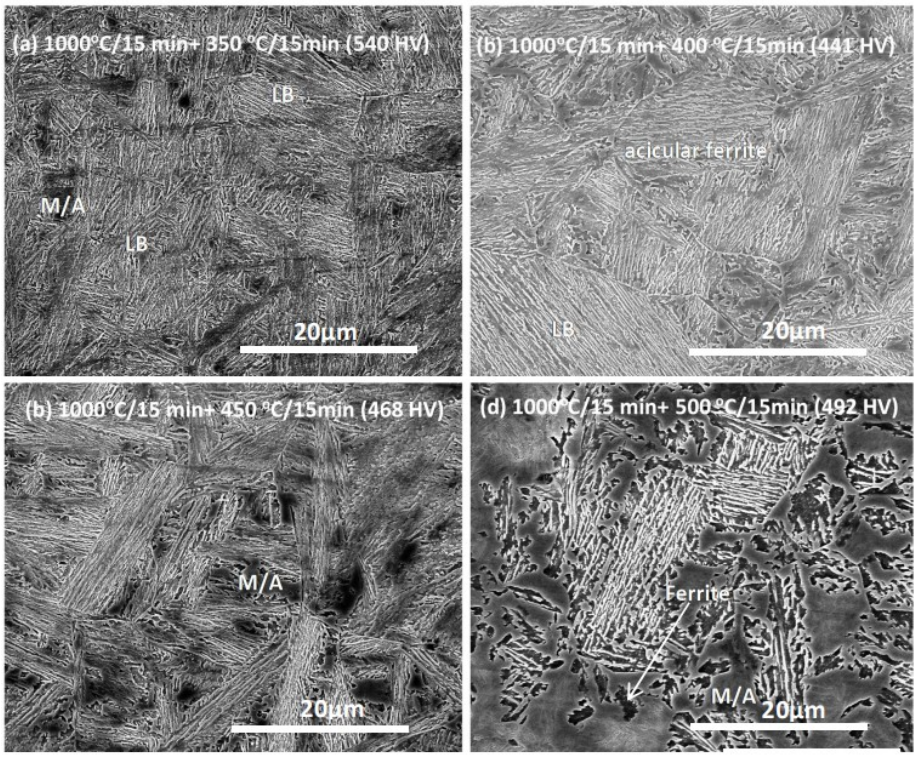

Figure 10. SEM micrograph of the steel in austenitized condition (1000ºC/15 min/ austempering for 30 min in salt bath at (a) 350ºC (b) 400 ºC (c) 450 ºC (d) 500 ºC

The XRD of the samples tested at various conditions is shown in Figure 11. The austenite content above A_{c3} temperature, has carbon content which is the overall carbon in the steel. During austempering, the austenite transforms to ferrite and carbide free retained austenite in a film form around ferrite laths. The bainitic carbide formation is suppressed by the presence of Si and hence a fine composite structure of soft ferrite with austenite film form a carbide free bainitic steel. The steel with such a microstructure is reported to show ultrahigh strength levels with excellent ductility. It is seen that the retained austenite content increases to a maximum value and decreases. At 500ºC austempering large blocky M/A constituents are seen. The marteniste content seem to be lower at around 400 ºC. It is also seen that the hardness value varies between 441 HV to 540 HV. The hardness value passes through a minimum at around 425 ºC austempering as per Figure 11. The hardness is lowered when the retained austenite content increases in the matrix.

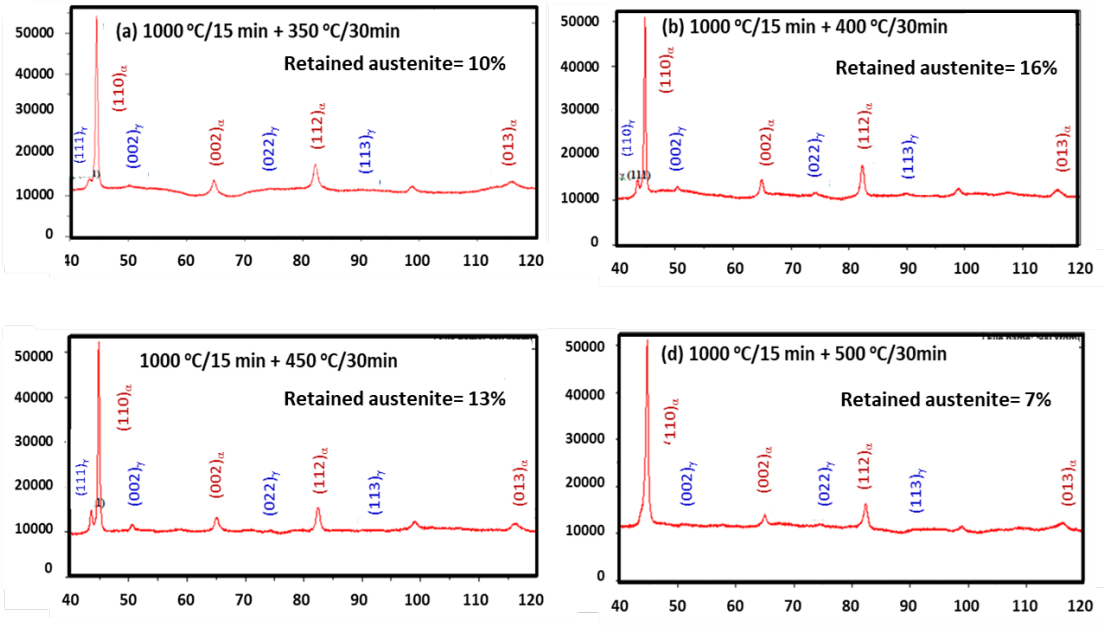

Figure 11. Carbide free bainitic steel shows retained austenite peaks on 1000 C/15 min/ austempering at (a) 350 ºC/30 min (b) 400 ºC/30 min (c) 430 ºC/30 min (d) 500ºC/30 min

3.6 Austempering After Intercritical Treatment / TRIP Assisted Steel

The austempering heat treatment carried out after initial austenitizing in the intercritical annealing temperature of 760 ºC followed by salt bath heat treatment between 350 and 500ºC at 50 ºC step, showed TRIP assisted microstructures of polygonal ferrite, bainitic ferrite, retained austenite and some M/A constituents. The optical microstructure obtained in the study is shown in Figure 12. Regions of dense bainitic sheaves along with islands of inter critical ferrite is observed. The SEM microstructures of the steel are shown in Figure 13. Acicular ferrite with dispersed bainitic ferrite and coarse carbides were observed. There are some regions of pearlite as well. At the intercritical temperature austenitization, the carbon partitions between ferrite and austenite results in carbon rich austenite. Further, austempering leads to the transformation of retained austenite to banitic carbide and retained austenite. The presence of polygonal ferrite decreases the hardness of the steel. The holding for 30 min duration has coarsened the bainitic ferrite to form fine carbide dispersion. In some regions, the retained austenite has transformed to pearlite in the steel. The microstructures show a complex distribution of ferrite with bainitic carbide, regions of pearlite and also some dense regions of martensite/austenite constituent. The hardness in the material varied between 256 to 293 HV and it peaks at around 425 ºC as shown in Figure 14. The XRD analysis on the samples shown in Figure 15, indicates ferrite peaks with no retained austenite. Thus, the ferrite with bainitic ferrite predominates the microstructure. At 425 ºC probably the bainite volume is highest as shown in Figure 5.

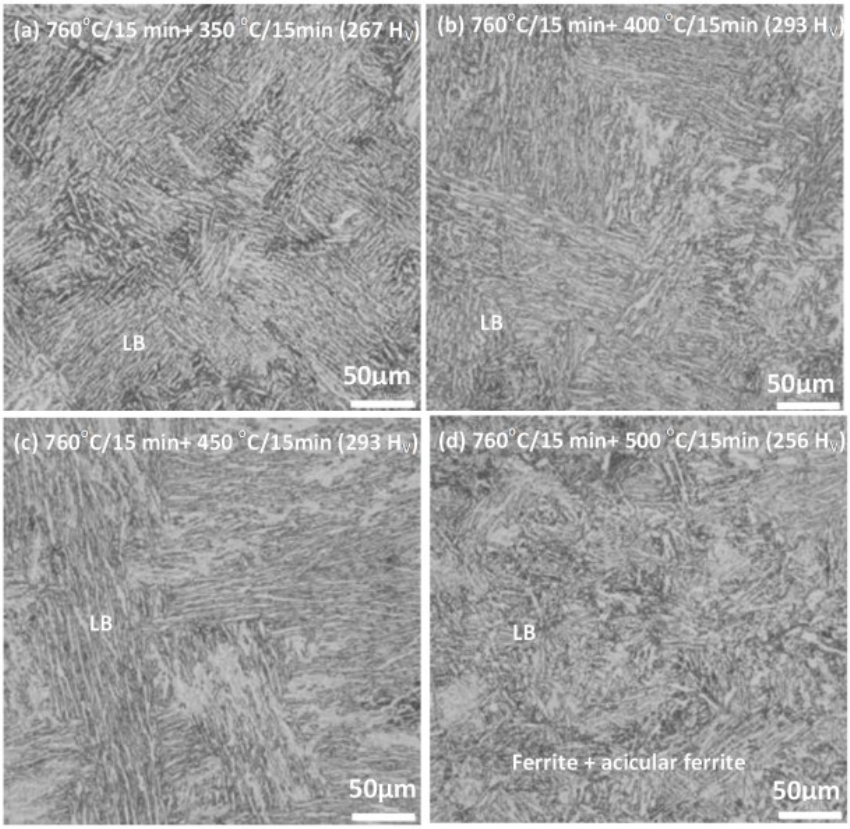

Figure 12. Microstructure of steel austenitized at 760 ºC/15 min/ austempering for 30 min in salt bath at (a) 350ºC (b) 400 ºC (c) 450 ºC (d) 500 ºC.

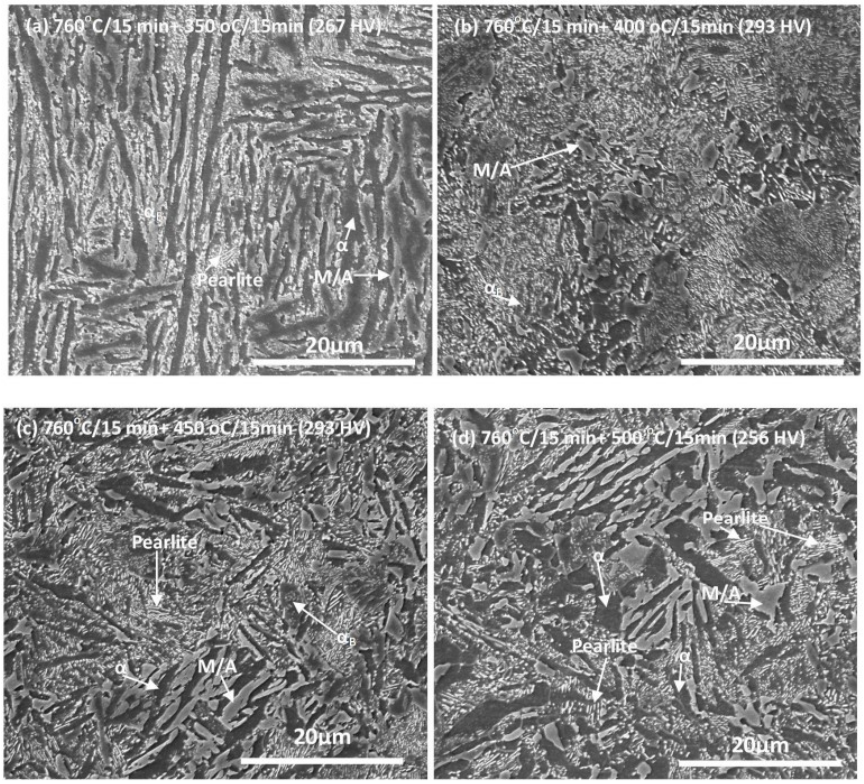

Figure 13. SEM micrographs of steel austenitized at 760 ºC for 15 min/ austempering for 30 min in salt bath at (a) 350ºC (b) 400 ºC (c) 450 ºC (d) 500 ºC

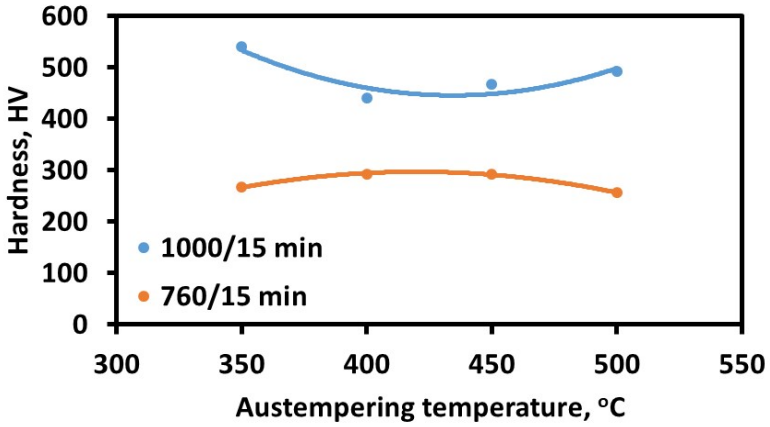

Figure 14. Hardness of the steel as a function of austempering temperature

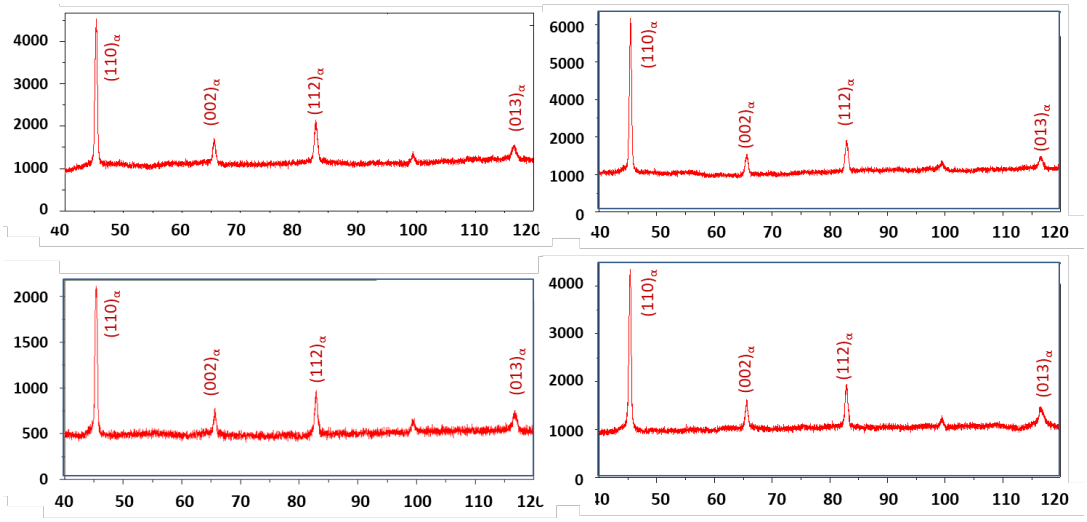

Figure 15. XRD of the steel austenitized at 760 ºC for 15 min/ austempering for 30 min in salt bath at (a) 350ºC (b) 400 ºC (c) 450 ºC (d) 500 ºC

4. Conclusions

- The microstructure evolution in a 0.38% C- 1.34 % Si-1.97 % Mn-0.8 % Cr-0.3% Mo steel was evaluated at various thermal processing conditions resulting in diverse range of microstructures.
- The steel on conventional annealing heat treatment produced a microstructure consisting of acicular ferrite and pearlite with a hardness of 277 HV.
- Normalising the steel from above Ac_3 resulted in ferrite, bainitic ferrite and retained austenite of 7% with a hardness of 349 HV.
- Normalizing the steel from the intercritical temperature range gave ferrite, bainitic ferrite and pearlite without retained austenite, with a hardness of 233 HV.
- Austenitizing above Ac_3 followed by austempering in a temperature range 350 to 500ºC showed development of carbide free bainitic microstructure with film of retained austenite and ferrite in lamellar form. The retained austenite content varied from 7 to 16% with presence of isolated blocky M/A constitutents. The hardness value varied from 441 to 540 HV.
- Austenitization in the intercritical range followed by austempering in the temperature range 350 to 500ºC showed formation of polygonal ferrite with baintic carbide and pearlite with isolated blocky M/A constitutents. The hardness value varied from 256 to 293 HV.

References

Arif Basuki and Etienne Aernoudt, (1999). *Scripta Mater,* 40, 1003.

B Masek, H Stan Kova, Z Novy, L W Meyer and A Kraci, (2009). *J. of Mater. Eng. and Perf.* 18, 385.

C Hofer, F Winkelhofer, J Krammerbauer, H Clemensa, S Primig, (2015). *Mater. Today: Proc.* 2S, S925.

C Hofer, H Leitner, F Winkelhofer, H Clemens, S Primig, (2015). *Mater. Charact.,* 102, 85.

F G Caballero, M J Santofimia, C Capdevila, C Garcia-Mateo and C G de Andres, (2006). *ISIJ Int*. DOI: 10.2355/isijinternational.46.1479.

F G Caballero, S Allain, J Cornide, J D Puerta Velasquez, C Garcia-Mateo, M K Miller, (2013). Mater. and Design, 49, 667.

G Gao, B Bai, H Zhang, X Gui, Z Tan and Y Weng, (2019). *Heat Treat. and Surf. Eng.,* 1, 1, DOI: 10.1080/25787616.2018.1560138.

H Asmari, E Emadoddin, A Habibolahzade, (2012). *Int. J. of Metall. Eng.,* 1, 66.

I Samajdar, E Girault, B Verlinden, E Aernoudt and J Van, (1998). *ISIJ Int.* 38**,** 998.

I Timokhina, E Pereloma, and P Hodgson, (2014). *Metall. And Mater. Trans. A*: DOI: 10.1007/s11661-014-2376-0.

J A Rodriguez-Martinez, R Pesci, A Rusinek, A Arias, R Zaera, D A Pedroche, (2010). *Int. J. of Solids and Struct.,* 47, 1268.

J C Hell, M Dehmas, S Allain, J M Prado, A Hazotte and J P Chateau, (2011). *ISIJ Int.,* 51, 1724.

J Trzaska, (2016). *Arch. Metall. Mater.,* 61, 981.

J Zrnik, O Muransky, O Stejskal, P Lukas and P Hornak, (2008). *Mater. Sci. and Eng. A,* 483–484, 71.

J Zrnik, O Muransky, P Lukas, Z Novy, P Sittner, P Hornak, (2006). *Mater. Sci. and Eng. A,* 437, 114.

J Zrnik, O Stejskal, Z Novy, P Hornak and M Fujda, (2007). *Mater. Sci. and Eng. A,* 462**,** 253.

K Hausmann, D Krizan, A Pichle, A Werner, (2013). *October 2013 Conference: Mater. Sci. and Techn. Conf. (MS&T) At: Montreal, Canada Project: TBF steels.*

K Sugimoto, A Kanda, R Kikuchi, S Hashimoto, T Kashima and S Ikeda, (2002). ISIJ Int. 42, 910.

L C Zhang, I B Timokhina, A La Fontaine, S P Ringer, P D Hodgson, E V Pereloma, (2009). *Memorie Acciaio, La Metall. Italiana, Giugno*, 49-55.

L Kucerova, M Bystriansky, (2016). *J. of Achiev. in Mater. and Manuf. Eng.,* 77**,** 5.

L Liu, B He and M Huang, (2018). *Adv. Eng. Mater.,* 1701083, 1.

M Breuer, M Degner, G Bader, W Bleck and F Morganti, (2017). *Technical contribution to the 54th Seminario de Laminacaoe Conformacao de Metais, part of the ABM Week, October 2nd -6th, Sao Paulo, SP, Brazil,* 28.

M E Mehtedi, S Spinarelli, J Zrnik, (2010). *Memorie Acciaio, La Metall. Italiana,* 10**,** 5.

M Zhou, G Xu, J Tian, H Hu and Q Yuan, (2017). *Metals,* 7, 263, doi:10.3390/met7070263.

MUCG83 Cambridge Univ software. https://www.phasetrans.msm.cam.ac.uk/map/steel/programs/mucg83.html.

O Muransky, P Hornak, P Lukas, J Zrník, P Sittner, (2006). *J. of Achiev. in Mater. and Manuf. Eng.,* 14, 26.

R Petrov, L Kestens, A Wasilkowska, and Y Houbaert, (2007). *Mater. Sci. and Eng. A,* 447, 285.

S Nemecek, Z Novy, H Stankov, (2006). Trattamenti Termici, La Metallurgia Italiana, 2, 47.

S Tang, H Lan, Z Liu and G Wang, (2021). *Metals,* 11, 96. https://doi.org/10.3390/met11010096.

S Wen, L Lin, B C De Cooman, P Wollants, Y Chun-xia, (2008). *J. of Iron and Steel Res.,* 15, 61.

T B Hilditch, I B Timokhina, L T Robertson, E V Pereloma, and P D Hodgson, (2009). *Metall. and Mater. Trans. A*, 40A**,** 342.

W Bleck, X Guo and M Yan, (2017). *Steel Res. Int.,* 88**,** 1.

Z P Xiong, A G Kostryzhev, L Chen, EV Pereloma, (2016). *Mater. Sci. & Eng. A,* 677, 356.